EUFAR ACAS Summer School
Scientific Report (Group 3)

Alberto Cazorla, Andreas Weigelt, Dina Santos, Emil Carstea, Jérôme Rangognio and Sabrina Melchionna

Group 3 flew on April 24, 2008. As we were the third group for the flight mission, we had the opportunity to get the experience of the previous groups for preparing our flight plan. We are a diverse group concerning scientific interests. Because of that we designed a heterogeneous experiment combining aerosol and cloud measurements, which were also the two main goals of the ACAS School.
Because the weather conditions and flight restrictions were favorable for our experiment, we followed the flight plan nearly step by step.

1. Aim of the flight

The aims of this flight were to investigate the aerosol and trace gases variability within the planetary boundary layer (PBL) between the Netherlands and south-eastern England and also to investigate the aerosol cloud interaction and cloud aging.

2. Flight preparation

According to a Sortie Brief one day before, the take off was planed for 0830 UTC (1030 LT) and the landing for 1050 UTC (1250 LT).
Analyzing the weather prediction, we expect to find a frontal system over south-eastern England (cf. Fig. 1).
The key instruments we want to use were all the aerosol and cloud particle counters, the PCASP/Nephelometer, the Constant flow Virtual Impactor (CVI), the Johnson Williams Liquid Water Content Probe, and the Nevzorov Liquid and Total Water Content Probe.
After take of at Rotterdam, for the first part of the experiment we planed to flight perpendicular to the wind direction. We intend to start at level 2500ft (for 10 min), then go down at level 1500ft (for 10min), continue to go down to 50 ft (for 15 min), make a profile at 1000ft/min during 5 min, and then fly for 10 min at level 5000 ft.
For the second part of our flight we planed to look for low/medium level clouds and do vertical profiling at three altitudes (10 min each): close below cloud base, 500ft above cloud base and 500ft below cloud top.
On the third part of our flight, we intend to climb at level 30000ft, drop a sonde and then fly back to Rotterdam.

3. Final flight

In terms of planning, the experiment went very well. We expected a frontal system and the forecast did not let us down. We had that frontal system located in the north coast of East Anglia and we had clear sky during the first part of the flight crossing the Southern North Sea.

The two main research areas were: firstly, measuring aerosol/plumes from South England sources perpendicular to the mean low-level flow across the southern North Sea and off the North Norfolk coast; and secondly, 'working' a water-cloud layer of Stratocumulus/Altocumulus, with runs above, in and below this cloud.

Instrumentation worked well, with few problems – SID 2 was unreliable (SID 1 worked OK), and less than usual warm-up time for the core instrumentation pre-take off (although no problems with core data subsequently).

The first section of the flight were flown exactly as planned, with a general track of 300 deg from Rotterdam towards the North coast of East Anglia, then westwards towards the Wash, being very much perpendicular to the mean low-level boundary layer flow of 210 deg, becoming 180 – 190 deg further west (cf. Fig. 2).

Next, we climbed and tried to select a suitable low/medium water cloud layer to examine. Although a good Stratocumulus/Altocumulus layer was found in the operating area, in reality it proved rather difficult to fly the required legs above, in and below this cloud layer. With some 'trial and error', and some rapid decision-making changes and updates, we managed to make the best out of this cloud situation with runs (each of an average of around 7 minutes) at:

(a) FL100, then FL 110 (run near cloud-top)
(b) FL140 (run above cloud top)
(c) FL 070 (run near cloud base) &
(d) FL 050 (run under cloud base).

Thereafter, we climbed to 19000 ft and then:

(a) Performed a 2g, 60 deg bank-angle orbit (rolling to the right) through about 270 deg, for radiometer calibrations.
(b) Dropped a sonde, which worked well, giving good met and wind data all the way down to the surface.

Finally, we recovered to Rotterdam, landing at 1049 UTC, after 2h 14 min flight duration.

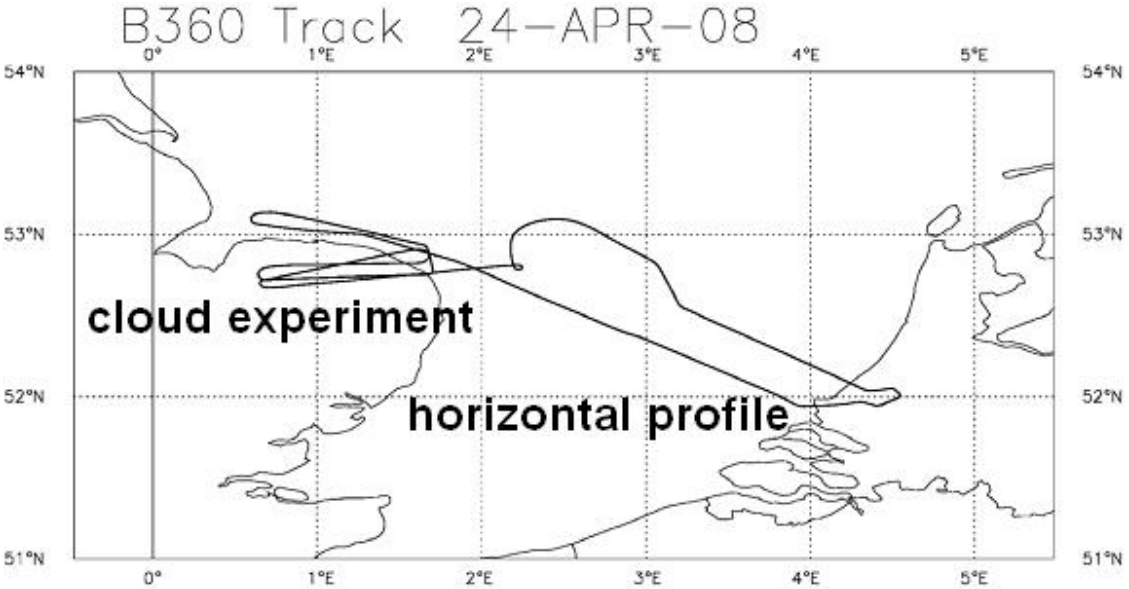

Figure 1. Flight track of the research flight on 24 April 2008 during the ACAS Summer School. Take off was at 08:34 UTC. The duration of the flight was 2h 15 min. The flight was divided into two parts: first obtaining a horizontal profile and second a cloud experiment.

Over the southern North Sea the visibility was generally good and deteriorating somewhat when we came closer to the frontal system over the North of East Anglia. The Cloud we chose for the cloud experiment grew somewhat while the measurements were performed. Some haze and low stratus was present over the Rotterdam area initially, soon dispersing. Cirrus/Cirrostratus cloud increased from small amounts near the Dutch coast to 8/8 cover near the Wash area. When flying towards the frontal system, layers of low and medium frontal cloud increased in thickness. The wind direction was generally S – SSW, with light to moderate wind speed at low level, increasing somewhat with increasing height. As it can be seen in Fig. 2, around one hour after landing the frontal system was located in front of the east coast of England.

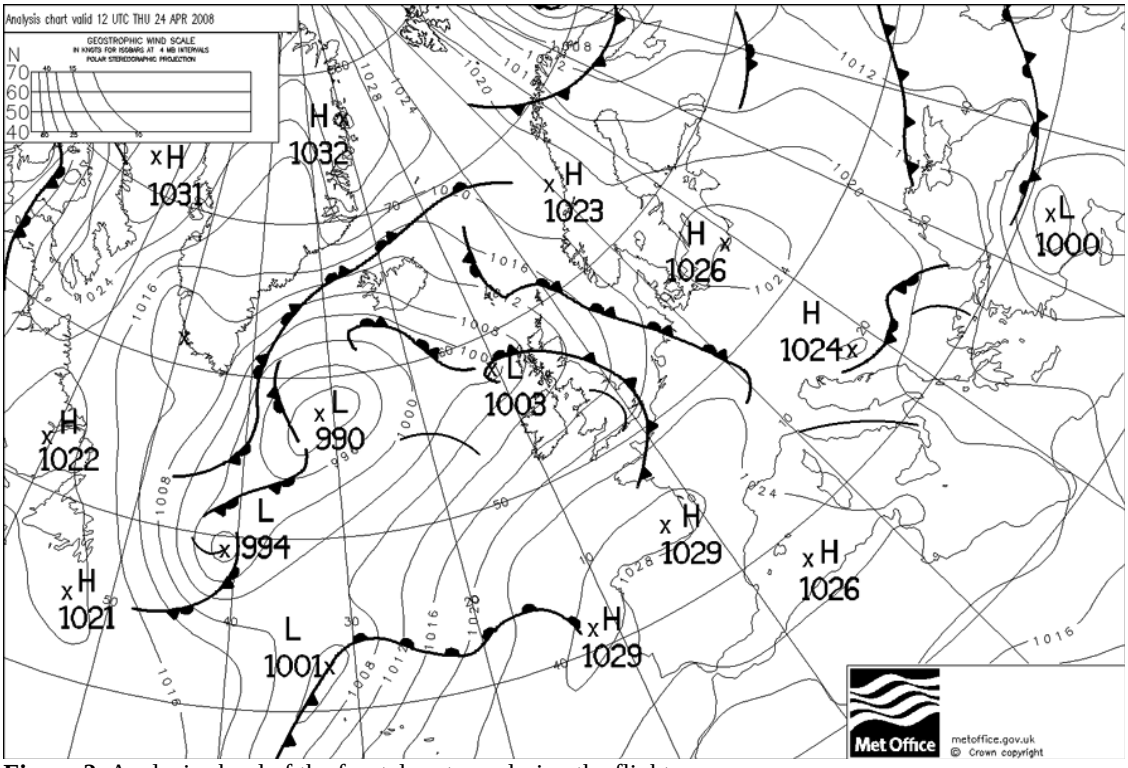

Figure 2. Analysis chard of the frontal systems during the flight.

4. Instruments used in data analysis

PCASP. Located in the PMS canister of the aircraft, the PCASP measures the size spectrum of aerosol particles between 0.1µm and 3µm in diameter. The core data product has a temporal resolution of 1-second and provides the aerosol particle concentration, the mean volume radius and the size spectrum (given in 15 bins).

Johnson Williams Liquid Water Content Probe. The Johnson Williams (JW) measures the concentration of liquid water in clouds using a heated wire resistance bridge. The operating range is 0.001 - 3 g/m3 and the sampling rate is 4 Hz. The time response is typically 1 s. The overall uncertainty under normal operation is estimated to be ±10%.

Nevzorov Liquid and Total Water Content Probe. The Nevzorov measures the concentration of liquid - and total (ice plus liquid) water in clouds. The operating range is between 0.003 gm^{-1} and 3 gm^{-1}. The sampling rate of that instrument is 8 Hz. The typical overall uncertainty under normal operation is also estimated to be ±10%.

CVI Constant flow Virtual Impactor. The CVI is a device designed by the University of Stockholm and the Met Office to collect cloud droplets by removing them from the airflow and evaporating the water to leave a residual particle and water vapor.

2D-P. Located in the PMS canister of the aircraft, the 2D-P measures the water droplet/ice crystal size spectrum (200µm < d < 6400µm). The core data products are 5-second averaged values of: particle number concentration, condensed water content, mean volume radius, precipitation rate and size spectrum (given in 32 bins to cover the nominal size ranges of 200-6400 µm diameter with 200 µm resolution). The particle diameter is determined from the shadow image using a single defined algorithm. This is probably the mean of maximum dimensions measured parallel and perpendicular to the detector array. The dimension perpendicular to the detector array is corrected for differences between the actual aircraft true airspeed and that used to set the probe clock rate. Condensed water content and precipitation rate is determined by calculating individual particle masses and fall speeds using specified functions of the particle diameter. There is an option to specify that the particle images are to be treated as either all ice or all liquid.

2D-C. Located in the PMS canister of the aircraft, the 2D-C measures the water droplet/ice crystal size spectrum (50µm < d < 800µm). The core data products are 5-second averaged values of: particle number concentration, condensed water content, mean volume radius, precipitation rate and size spectrum (given in 32 bins to cover the nominal size ranges of 25-800 µm diameter with 25 µm resolution). The particle diameter is determined from the shadow image using a single defined algorithm. This is probably the mean of maximum dimensions measured parallel and perpendicular to the detector array. The dimension perpendicular to the detector array is corrected for differences between the actual aircraft true airspeed and that used to set the probe clock rate. Condensed water content and precipitation rate is determined by calculating individual particle masses and fall speeds using specified functions of the particle diameter. There is an option to specify that the particle images are to be treated as either all ice or all liquid.

5. Data analysis

To get a uniform and comparable data set, the measured particle size distribution along the whole flight was converted to standard conditions (1013.25 hPa, 273.15 K). Figure 3 shows the particle size distribution along the whole flight route. In that graph, the color represents the number concentration at each particle size (please note the logarithmic scale at the particle size and the concentration). The increased particle concentration in nearly all size channels smaller than 1 µm after 10:42 UTC (38500 sec) might be caused by the contaminated air around Rotterdam airport. All the other results from the PCASP will be discussed for the two parts of the flight separately. The first part (horizontal aerosol profile between the coast of the Netherlands and south-east England) took place between 08:41 UTC (31260 sec) and 09:32 UTC (34320 sec). The second part (cloud experiment) began at 09:37 UTC (34620 sec) and ended at 10:13 UTC (36780 sec).

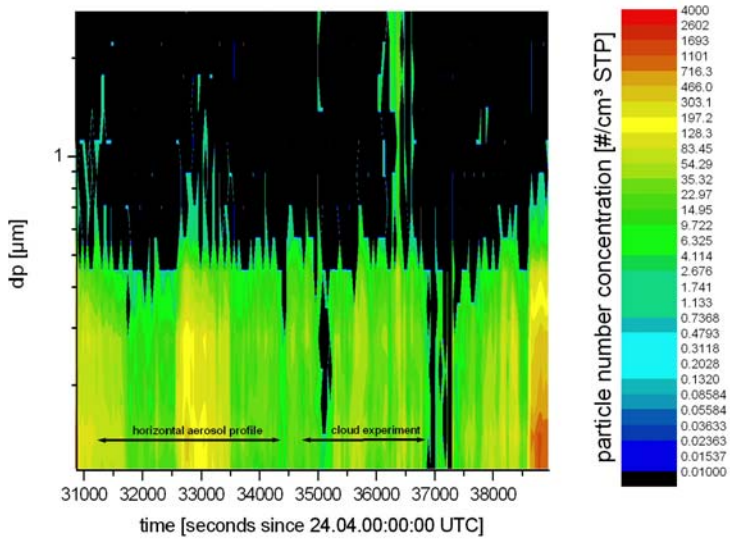

Figure 3. Particle size distribution measured with the wing borne PCASP along the whole flight track. The color represents the number concentration at each particle size. All concentrations were converted to standard conditions (1013.25 hPa, 273.15 K). Concentrations below 0.01 #/cm³ STP are shown in black. Blue bars show the runs being identified inside the cloud and green bars show the outside cloud runs

5.1 Horizontal aerosol profile

During the first part of the experiment the measurements were obtained on a flight route perpendicular to the wind direction. In the same manner as in Fig. 3, Fig. 4 shows the particle size distribution, but only for the first part of the flight. Please note the different scale for the particle concentration, compared to Fig. 3. Between 08:41 UTC (31260 sec) and 08:49 UTC (31740 sec) the concentration of particles smaller than 0.4 µm in diameter (d_p) seems to be somewhat increased, compared to the measurements from 08:49 UTC to 09:03 UTC (32580 sec). This increase might be caused by the industry along the Dutch coast. As it can be seen in Fig. 4, between 09:03 UTC and 09:19 UTC (33540 sec) the concentration of nearly all particle sizes was significantly increased up to 1000 particles/cm³ STP.

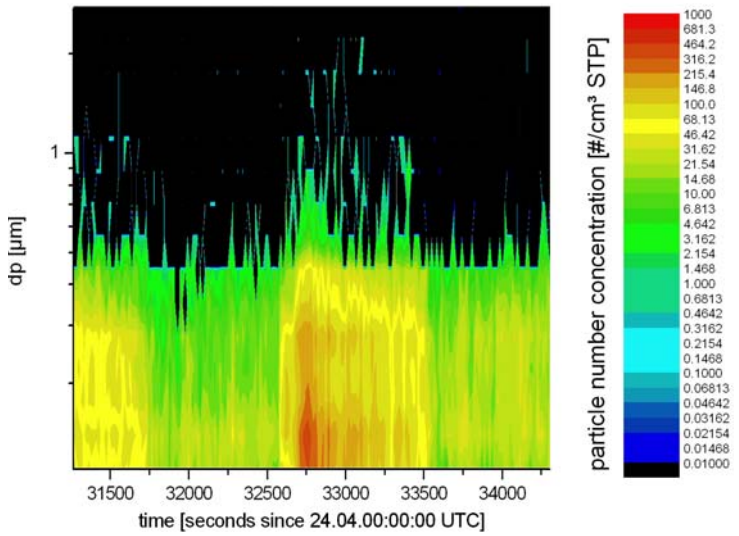

Figure 4. Particle size distribution like in Fig.3, but only for the horizontal aerosol profile. Please note the different scale for the particle concentration.

Thereafter the analyzed air masses had a much lower maximum particle concentration (up to 68 particles/cm³ STP within each size channels of the instrument). However, from 09:17 UTC (33420 sec) to the end of that plot probably the same air mass was measured as in the 15 minutes before, but in a much higher altitude. This is, because at 09:17 UTC the aircraft turned around, climbed to ~1550 m, and fly the same way back (see Fig. 1). To analyze the origin of the polluted air mass between 32580 sec and 33540 sec, 12 hour backward trajectories were calculated using the NOAA HYSPLIT trajectory model (http://www.arl.noaa.gov/ready/hysplit4.html). The backward trajectories were calculated in three altitudes and at two positions along the flight track of the aircraft (Fig. 5). The first starting point (1) was chosen where the not polluted air mass was measured (52.4°N, 3.0°E). The second starting point (2) was set to 53.0°N, 1.4°E, where the polluted air was measured. For each point the backward trajectories started at 80m, 800m, and 1540m. During the measurement of the not polluted air masses between 31740 sec and 32580 sec, the cruising altitude of the aircraft was ~800m and hence the red backward trajectory starting at (1) indicates the origin of the air mass over the English Channel. The measurements of the polluted air masses were taken at an altitude of ~80m. So the blue backward trajectory starting at (2) shows that those air masses directly crosses London. Hence, contrary to the “clean” air masses between 31740 sec and 32580 sec, the air masses between 32580 sec and 33540 sec were most likely contaminated by the London plume. However, also the air masses measured after 33420 sec crosses London (green backward trajectory starting at (2)), but show no significant higher particle concentrations compared to the air masses analyzed at position (1). As the measurements were taken above the boundary layer at an altitude of ~1550m, also over London the analyzed air masses were above the boundary layer (see Fig. 5). Hence, the analyzed air masses were only slightly contaminated by the London plume.

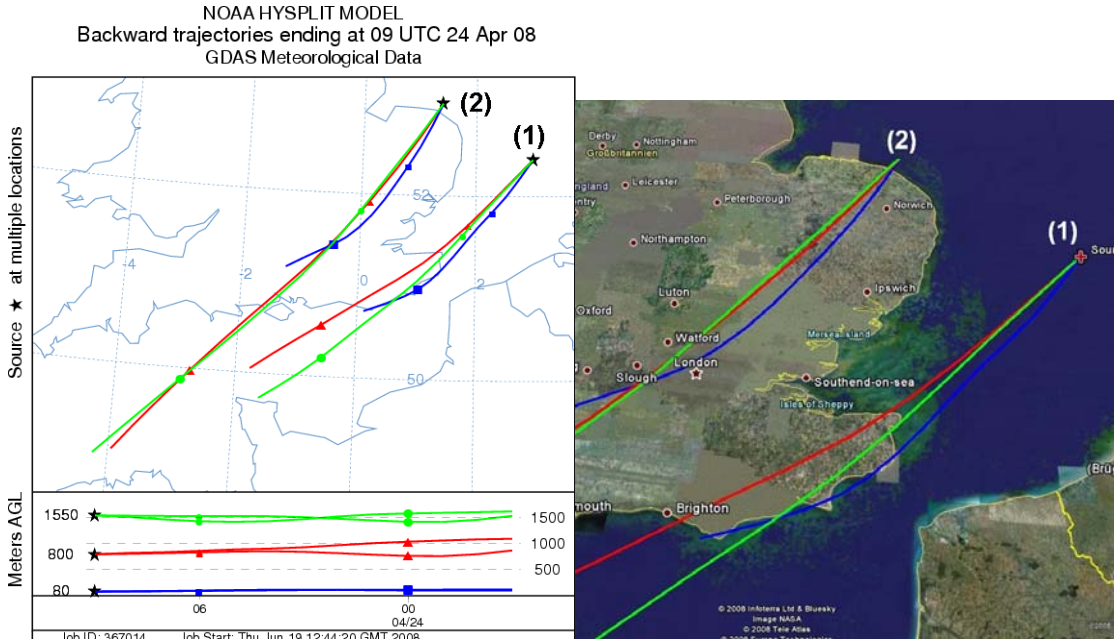

Figure 5. 12 hour backward trajectories, calculated with the NOAA HYSPLIT trajectory model along the flight track of the aircraft (http://www.arl.noaa.gov/ready/hysplit4.html). The start points were set to 52.4°N, 3.0°N (1) and 53.0°N, 1.4°E (2). At both positions the backward trajectories start at an altitude 80m (blue), 800m (red), and 1550m (green).

5.2 Cloud experiment

In the second part of the experiment the influence of a Stratocumulus/Altocumulus cloud on the aerosol particle size distribution was analyzed. This cloud was located inside a frontal system over south-east England (see Fig. 2). Measurements were enforced close below the cloud base, shortly above the cloud base, inside the cloud top, and above the cloud top. To determine, at which time the measurements were taken inside/outside the cloud, we used the camera data, as well as the Liquid Water Content (LWC) as indicator. The LWC was measured with the Johnson Williams liquid content probe (JW) and in parallel with the Nevzorov probe. The first run of that experiment was identified to take place inside the cloud top at about 3400 m above sea level between 09:37:32 UTC (34652 sec) and 09:44:46 UTC (35086 sec) (Fig. 6). After turning around and changing the altitude, the second run from 09:47:00 UTC (35220 sec) to 09:53:56 UTC (35636 sec) was above the cloud top at ~4300 m above sea level. The third run from 09:57:00 UTC (35820 sec) to 10:06:01 UTC (36361 sec) was inside the cloud base (~2200 m above sea level) and the fourth run (10:09:20 UTC; 36560 sec to 10:13:13 UTC; 36793 sec) was below the cloud base (~1600 m above sea level).

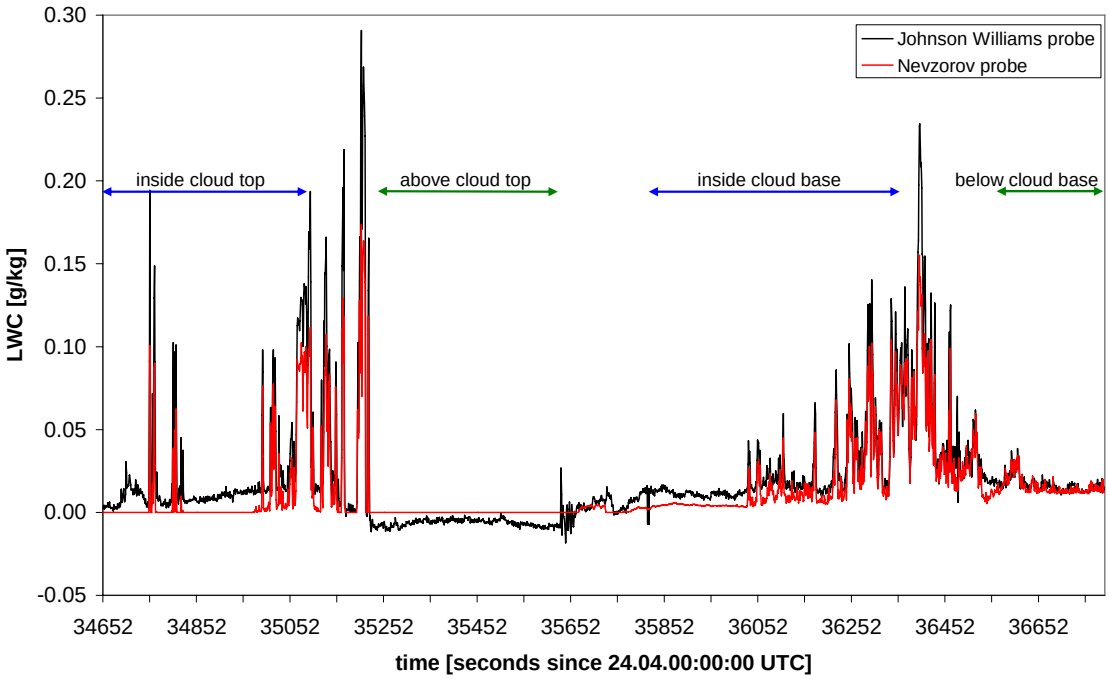

Figure 6. Liquid Water Content measured during the cloud experiment with the Johnson Williams and the Nevzorov liquid content probe. Blue bars show the runs being identified inside the cloud and green bars show the outside cloud runs. For the inside/outside cloud decision, also the video data were analyzed. After each run the aircraft changed the altitude

Figure 7 shows the particle size distribution, measured during the whole cloud experiment. Through the whole cloud the concentration of particles larger than 0.5 µm is nearly zero. Additionally it can be seen that there is no significant increase/decrease of the concentration in a specific layer, compared to the other layers. Only above the cloud top the concentration of particles smaller than 0.2µm seems to be somewhat increased. However, an increased particle number concentration was observed in nearly all size channels during the vertical movements of the aircraft. Especially between the runs three and four (inside and below the cloud base) the concentration of particles larger than 0.5 µm was significantly increased. On the contrary, between the second and the third run only the concentration of particles smaller than 0.5 µm was increased. This increased concentration between the runs could be due to errors of the instrument when changing the pressure level rapidly. Hence, one has to be careful when interpreting these data. Because of that we did not analyzed this intermediate data.

To quantify the overall influence of the cloud on the particle size distribution, the measurements were averaged within each run. Figure 8 shows the mean and median particle size distributions, obtained below, within, and above the analyzed cloud. In all four altitudes in Fig. 8a the accumulation mode (0.1 µm d_p 1µm), as well as the coarse mode (1 µm d_p) can be clearly identified. However, for particles larger than 0.45 µm, the median concentration becomes zero within each altitude (Fig. 8b). This behavior indicates that the means are increased by few high concentrations, whereas at the majority of the measurements no particles occurred with d_p 0.45 µm.

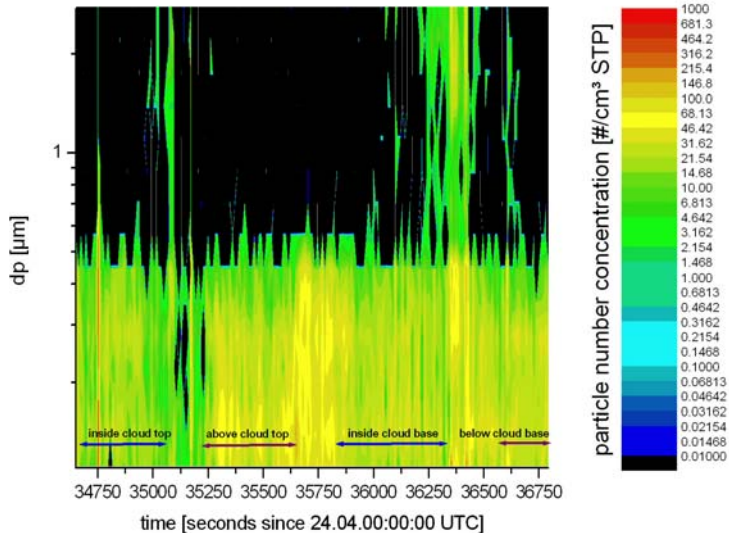

Figure 7. Particle size distribution like in Fig. 2, but only for the cloud experiment. Blue bars show the runs being identified inside the cloud and green bars show the outside cloud runs. Please note the different scale for the particle concentration.

Comparing the averaged particle size distributions of the different altitudes to each other, a small difference becomes apparent. Please note the logarithmic scales at both axes. As it can be seen in Fig. 8, within the Accumulation mode the mean and median concentration inside the cloud top was reduced by about 40 % compared to the concentration in the other altitudes (e.g. above the cloud top). On the contrary in the coarse mode, the mean concentration above the cloud top was significantly lower than the other altitudes. However, as it is also obvious in Fig. 7, the concentration of coarse mode particles was almost zero during the whole measurement time above the cloud top. Hence, the mean value is originated by only few occurrences of coarse mode particles in that altitude.

These differences in the particle size distribution might be caused by the influence of the cloud on the aerosol particles. As a cloud indicates an upward-welling air motion (e.g. due to convection or inside a frontal system), aerosol particles as well as particle precursor gases were transported from the boundary layer through the cloud to their outflow region. Along this way the cloud can act as a sink for particles by activating them to cloud droplets and precipitation. Moreover the cloud can vertically transport aerosol particles in their updraft and can act as a source for new particles by preferring binary homogeneous nucleation [e.g., Perry and Hobbs, 1994; Zhang et al.,1998; Ström et al., 1999; de Reus et al., 2001; Weber et al., 2001, Ekman et al., 2006; Kanawade and Tripathi, 2006; Weigelt et al., 2008]. Because the lower detection limit is around 0.1 µm, the formation of new particles could be not observed with the used PCASP system.

The particle size distribution below and within the cloud base did not differ significantly. This less difference indicates that not as much particles were activated in the cloud base where our measurements took place. However, comparing the Accumulation mode concentration at the cloud top to that at the cloud base, the mean and median values were approximatively 40 % lower inside the cloud top (Fig. 8a). This less high concentration is most likely due to the activation of many particles to cloud droplets during their transport to the cloud top. On the contrary, no difference to the concentration

of the former altitudes was obviously due to the coarse mode particles inside the cloud top. As the occurrence of coarse mode particles was really low, this result might be not significant. Above the cloud top the concentration of Accumulation mode particles was similar to the concentration at the cloud base. This might be caused by evaporating the cloud droplets in the outflow region. In that manner the cloud reemits the remaining cores of the evaporated cloud droplet into the free troposphere. However, in that altitude the mean coarse mode concentration was nearly 80 % below the concentration in the other measurement levels. As the chosen cloud was a Stratocumulus/Altocumulus, the vertical wind speed inside the cloud might be not as high to transport coarse mode particles into the outflow region. But again, because of the fewer occurrences of coarse mode particles, this theory is very speculative and the finding might be not representative. Nevertheless it is a possible explanation for the observed particle size distribution.

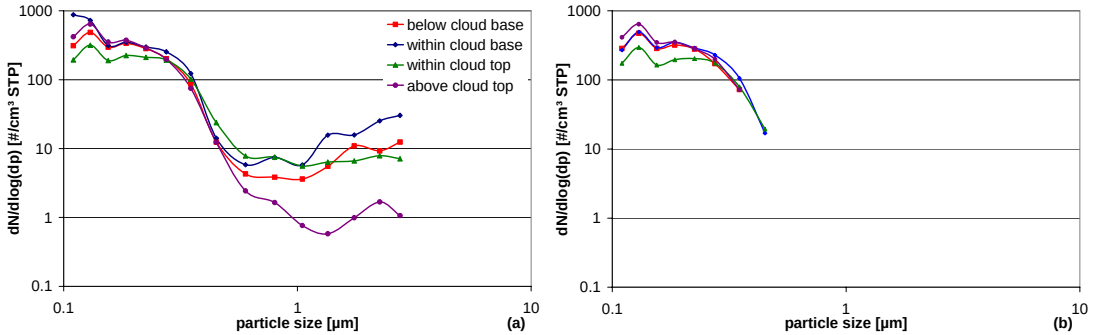

Figure 8. Particle size distribution, averaged over each run of the cloud experiment. The mean values are shown in (a) and the median values are shown in (b). All concentrations were converted to standard conditions (1013.25 hPa, 273.15 K). Concentrations of zero particles are not shown in the graphs.

As already hinted above, the chosen cloud was not the ideal one to study the influence of clouds on the aerosol particle size distribution, because of the less vertical wind speed inside this type of cloud. For this kind of analysis we would prefer a deep convective cloud with a much larger extend and a much higher vertical wind speed. As the number concentration of the atmospheric aerosol is dominated by particles smaller than 0.1 µm, it would be desirable to measure the particle size distribution starting at the nucleation mode ($d_p \leq 0.01$µm). In that way also the influence of clouds on the formation of new particles could be analyzed. Unfortunately there was no instrument onboard the aircraft providing this information (e.g. a scanning mobility particle sizer; SMPS).
During the whole experiment the particle size distribution was also recorded with a second PCASP system in combination with a Counterflow Virtual Impactor (CVI). In the following the system is called “CVI-PCASP”. As it was planed to operate the CVI in aerosol mode during the cloud experiment, the data should be comparable to the wing borne PCASP system. Unfortunately the settings of the CVI were changed several times during the cloud experiment. Because of that we cannot use these data to answer the question of the influence of the cloud on the particle size distribution. The same way as in Fig. 7, Fig. 9 shows the particle size distribution obtained with the CVI-PCASP. As it can be seen, the size distributions completely differ from each other. On the basis of Fig. 9 some changes in the settings of the CVI can be identified. At 09:37:39 UTC (34659 sec) the pressure pump of the CVI was switched off. As a result within 40 seconds the

concentration in all channels increases from zero up to 200 particles/cm³ STP. The pressure pump was switched on at 09:54:40 UTC (35680 sec) resulting in significant an increased concentration of particles between 0.11 µm and 0.16 µm in size. The variations in the particle concentration (mainly at $d_p \leq 0.2$ µm) between 10:02:24 UTC (36144 sec) and 10:09:19 UTC (36559 sec) might be caused by the reduction of the flow value. Because of these changes in the settings of the CVI, we did not analyze the CVI-PCASP data in more detail.

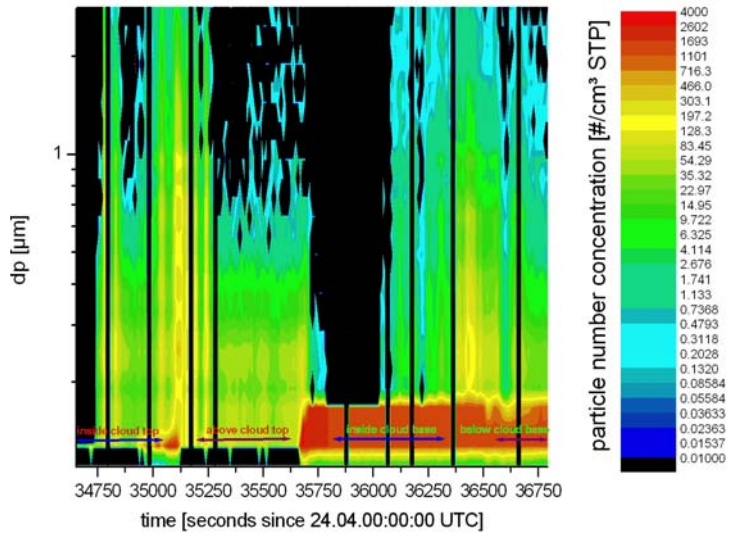

Figure 9. Particle size distribution during the cloud experiment like in Fig. 3, but for the CVI-PCASP system.

During the in-cloud runs, we also looked for the occurrence of different habits of cloud particles in the images, collected by the 2DC- and the 2DP probe. The particle imaging in these probes was obtained enlightening the particles with a laser beam, and projecting its shadow on a linear array of 32 photo detectors each. The output of the probe is composed by black and white discrete images. The 2DC and the 2DP have a resolution of 25 µm and 200 µm, respectively.

We related the different habits, recognized by eye following the classification schema of Korolev et al. [2000], with the temperature at the flight level and with the depth of the cloud (Fig. 10).

At the cloud top the distribution of the cloud particles was dominated by irregular crystals. Contrary, when flying inside the cloud base, large stellar crystals as well as needles were detected. During the last run below the cloud base, again little irregular crystals were recognized. Spherical particles were observed outside the cloud layer.
You can note that when we flew through the cloud base, the temperature was about -4°C. This temperature is favorable for the throw off of secondary ice crystals from rimed ice dendrites and is called Hallett and Mossop mechanism [Hallett and Mossop, 1985].. However, also the presence of super cooled cloud droplets is necessary to produce this splintering. If we looking at the liquid water content, registered by the Nezerov probe

(Fig. 6), the presence of liquid water between 9:55 and 10:15 UTC (35700 sec and 36900 sec, respectively) can be seen.
Also during the first run in the cloud top between 9:32 and 9:42 UTC (34320 sec and 34920 sec, respectively) cloud water was available. However, the temperature in that region was about -10°C and hece too low to produce splintering.
The observation of both, dendrites and needles in the conditions mentioned above, might be an indication for the multiplication of ice crystals observed in laboratory by Hallett and Mossop.

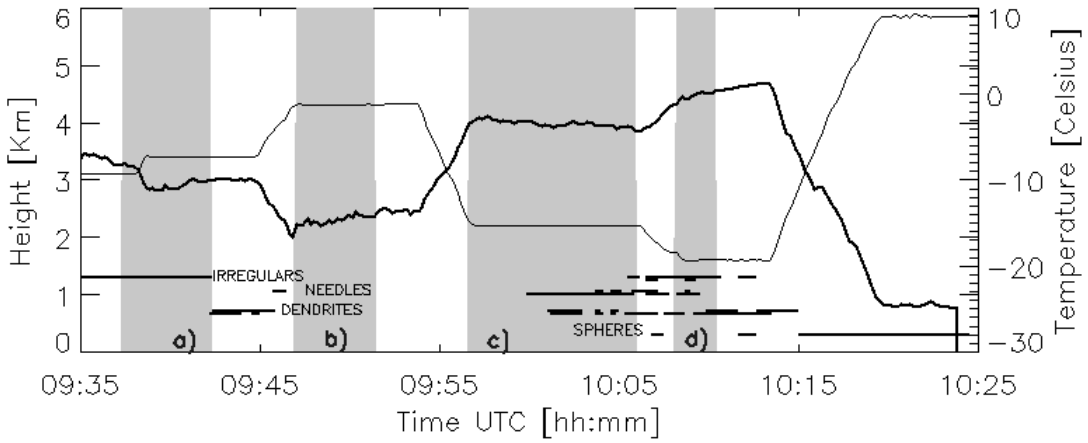

Figure 10. Changes of cloud particle habits during the flight B360 on 24 April 2008. Solid thin line: altitude; solid thick line: temperature; horizontal lines: presence of a kind of crystal habit (irregular, needle, dendrite or sphere); shadowed areas: a) inside cloud top; b) partially above cloud; c) above cloud base; d) partially below cloud base.

6. Final Considerations

The main objectives of this flight were to analyse the aerosol and trace gases variability within the PBL and also to investigate the aerosol cloud interaction and cloud aging.
In terms of flight planning and objectives, the experiment went very well. We measured aerosol/plumes from South England sources across the southern North Sea and off the North Norfolk coast. Furthermore we study a cloud layer of Stratocumulus/Altocumulus with runs above, in, and below this cloud. In the majority, the instrumentation worked well, with only a few problems. Even so we were able to use all the instruments we planed.
The first part of the flight was flown exactly as planned. Although a good Stratocumulus/Altocumulus layer was found in the operating area, actuality it proved somewhat difficult to fly the required altitude above, in and below this cloud layer. But, with some ‘trial and error’, and some rapid decision-making changes, we managed to make the best out of this cloud situation.
In the second part of the experiment the influence of a Stratocumulus/Altocumulus cloud, which was located inside a frontal system as we expect, on the aerosol particle size distribution was analyzed. The results are very interesting but a more completely study

(with some measurements from other instruments that were not accessible) is necessary to be able to take some accurate pronouncements.
In general the experiment was extremely good and our experience in training on airborne instrumentation, measurement, data analysis and interpretation was very successful.

Acknowledgements
We would like to thank EUFAR for supporting the school and for providing us such wonderful experience.

References

de Reus, M., R. Krejci, J. Williams, H. Fischer, R. Scheele, and J. Ström (2001), Vertical and horizontal distributions of the aerosol number concentration and size distribution over the northern Indian Ocean, J. Geophys. Res., 106 (D22), 28,629 - 628,641, doi: 0148-0227/0101/2001JD900017.

Ekman, A. M. L., C. Wang, J. Ström, and R. Krejci (2006), Explicit Simulation of Aerosol Physics in a Cloud-Resolving Model: Aerosol Transport and Processing in the Free Troposphere, J. Atmos. Sci., 63, 682–696, doi: 610.1175/JAS3645.1171.

Kanawade, V., and S. N. Tripathi (2006), Evidence for the role of Ion-induced particle formation during an atmospheric nucleation event observed in Tropospheric Ozone Production about Spring Equinox (TOPSE), J. Geophys. Res., 111, D02209, doi: 02210.01029/02005JD006366.

Korolev, A., G. A. Isaac, and J. Hallet (2000), Ice Particles Habits in Stratiform Clouds, Q.J.R. Meteorol. Soc., pp. 2873-2902.

Mossop, S. C. (1985), The Origin and Concentration of Ice Crystal in Clouds, Bull. Am. Meteorol. Soc., pp.264-273.

Perry, K. D., and P. V. Hobbs (1994), Further evidence for particle nucleation in clear air adjacent to marine cumulus clouds, J. Geophys. Res., 99 (D11), 22.803-822.818, http://www.agu.org/pubs/crossref/1994/ 1994JD01926.shtml.

Ström, J., H. Fischer, J. Lelieveld, and S. F. (1999), In situ measurements of microphysical properties and trace gases in two cumulonimbus anvils over western Europe, J. Geophys. Res., 104 (D10), 12,221–212,226.

Weber, R. J., G. Chen, D. D. Davis, R. L. Mauldin, D. J. Tanner, F. L. Eisele, A. D. Clarke, D. C. Thornton, and A. R. Bandy (2001), Measurements of enhanced H2S04 and 3-4 nm particles near a frontal cloud during the First Aerosol Characterization

Experiment (ACE 1), J. Geophys. Res., 106 (D20), 24,107 124,117, doi: 110.1029/2000JD000109.

Weigelt, A., M. Hermann, P. F. J. van Velthoven, C. A. M. Brenninkmeijer, G. Schlaf, A. Zahn, and A. Wiedensohler, Influence of clouds on aerosol particle number concentrations in the upper troposphere, revised to J. Geophys. Res., (2008JD009805R)

Zhang, Y., S. Kreidenweis, and G. R. Taylor (1998), The Effects of Clouds on Aerosol and Chemical Species Production and Distribution. Part III: Aerosol Model Description and Sensitivity Analysis, J. Atmos. Sci., 55(6), 921-939.